World Academy of Science, Engineering and Technology
International Journal of Materials and Metallurgical Engineering
Vol:9, No:1, 2015

Numerical Simulation of Fiber Bragg Grating Spectrum for Mode-I Delamination Detection

O. Hassoon, M. Tarfoui, A. El Malk

***Abstract*—**Fiber Bragg optic sensor is embedded in composite material to detect and monitor the damage that occurs in composite structures. In this paper, we deal with the mode-I delamination to determine the material strength to crack propagation, using the coupling mode theory and T-matrix method to simulate the FBGs spectrum for both uniform and non-uniform strain distribution. The double cantilever beam test is modeled in FEM to determine the longitudinal strain. Two models are implemented, the first is the global half model, and the second is the sub-model to represent the FBGs with higher refined mesh. This method can simulate damage in composite structures and converting strain to a wavelength shifting in the FBG spectrum.

***Keywords*—**Fiber Bragg grating, Delamination detection, DCB, FBG spectrum, Structure health monitoring.

I. Introduction

THE delamination affects strongly the resistance capabilities of composite materials, however, it is difficult to be detected because it takes place inside structure and often being barely. Delamination is considered as one of the major failure mechanisms in laminated composites. This takes place among the plies or edges and occurs under different loadings such as impact and fatigue, makes it more dangerous in critical structures such as aircraft [1]. Fiber Bragg grating sensor (FBGs) is one of the new technologies adapted to detect and monitor damages in composite structures. FBGs offer the ability to be integrated inside of the structure due to its small size, and grace its multiplexing capability to detect the damage in several locations along a single fiber with immunity to magnetic fields effect.

The FBG embedding position and orientation must be selected corresponding to the load applied direction and along the axial direction of the reinforced fibre to avoid appearance of multi peaks in spectral response of FBG sensor [2]. FBGs spectrum can be simulated using the coupling theory and T-matrix method that were applied successfully to uniform and non- uniform strain distribution. Simulation of dynamic strain distribution along a uniform FBG aims to construct the reflected spectrum under three strain profiles: uniform, linear and quadratic strain gradient by applying the T-matrix method [3]. Small fiber Bragg grating sensors (FBGs) are used to detect the delamination in carbon reinforced plastic (CFRP) by measuring the reflected spectrum of the optical fiber among many delamination lengths in four-point bending test based on the intensity ration ratio of the reflected spectrum which is considered as an effective indicator to predict delamination lengths. Based on the strain distribution along the positions of the FBG [4], finite element method was used to simulate the reflected spectrum. Non-uniform strain distribution measurement induced by delamination propagation in mode-I delamination and identification of the bridging tractions in double cantilever beam (DCB) are applied for an uniaxially reinforced composite material, optical low–coherence reflectometry (OLCR) technique is used to overcome situation of the non-uniform strain distribution along FBGs grating [5]. Behzad studied the effect of (scaling bridging) the thickness to fracture of unidirectional glass fiber reinforced polymer (GFRP) for DCB test using embedded short FBGs with an array of eight or ten division multiplexing optical fiber Bragg to overcome the non-uniform strain distribution along the grating gauge [6]. Another author used the short grating length and multiplexing arrays to overcome the non-strain distribution along the FBG which is able to determine the local strains close to damage or crack plane to study the fracture of unidirectional carbon fiber /epoxy in DCB test under monotonic and fatigue loads [7].

In this research we built the coupling mode theory with the T-matrix method in Matlab codes to simulate the reflected spectrum of the FBG and the delamination induced by finite element method under Abaqus V 6.12, then we calculated the strain along the gauge of the FBG sub-model and transformed these information to Matlab code to construct the corresponding wavelengths shifting.

II. Uniform Strain and Temperature Distribution along Fiber Bragg Grating

The response of the FBG spectrum is based on the change in axial grating period and the refractive index. If these physical characteristics suffer under axial load and temperature, the shift of the wavelength will be uniform and the spectrum shape will not split. A very important advantage of an FBG sensor with encoded wavelength is the shifts in the spectrum that appear as a reflection narrowband or a dip in transmission which are independent of the optical intensity, but associated uniquely to each grating without overlap in each sensor stop-band. With care in selection of the Bragg wavelengths, each tandem array of FBG sensors registers only a measured change along its length and not from adjacent or distant transducers [8].

According to the Bragg's law, the wavelength can be calculated by:

O. Hassoon is with the ENSTA Bretagne /Brest/France (phone: +33668600885; e-mail: omar_hashim.hassoon@ensta-bretagne.fr).
M. Tarfoui is with the ENSTA Bretagne /Brest/France (phone: +33298348705; e-mail: mostaphatarfaoui/ensta_Bretagne@CAMPUS).

$$\lambda_b = 2n_{eff}\Lambda \quad (1)$$

where λ_b is the Bragg wavelength, n_{eff} and Λ are respectively the average refractive index and the grating period. The change in the wavelength depends on the change in physical properties of the optical fiber grating such as change in the local period and reflective index along the fiber gauge.

$$n_{eff} = n_0 - \frac{n_0^3}{2}[p_{12} - v_f(p_{11} + p_{12})\varepsilon_z] \quad (2)$$

$$\Lambda = (1 + \varepsilon_z)\ \varepsilon_0 \quad (3)$$

Here n_0 and Λ_0 are respectively the initial average refractive index and the initial grating period, in a strain-free state. p_{11}, p_{12} are optical strain constants, and v_f is Poisson's ratio of the optical fiber.

The shift in Bragg wavelength when the temperature is constant can be expressed as:

$$\frac{\Delta\lambda_{b,x}}{\lambda_{b0}} = \varepsilon_z - \frac{n_0^2}{2}\left(p_{11}\varepsilon_x + p_{12}(\varepsilon_y + \varepsilon_z)\right) \quad (4)$$

$$\frac{\Delta\lambda_{b,y}}{\lambda_{b0}} = {}_z - \frac{n_0^2}{2}\left(p_{11y} + p_{12}({}_x + {}_z)\right) \quad (5)$$

Whereε_y, ε_x and ε_z are the principal strain components of the fiber core. The mean elongation in the structure is in the same axial direction of the optical fiber. The peak separation $\Delta\lambda_{b,y}$ - $\Delta\lambda_{b,x}$ only depends linearly on the transversal strains difference $\varepsilon_y - \varepsilon_x$. Assume that the glass fiber is isotopic (i.e. ε_y, ε_x are equal), a simplified equation can be obtained by averaging relations (4), (5).

$$\frac{\Delta\lambda_{b,y}}{\lambda_{b0}} = \varepsilon_z - \frac{n_0^2}{2} + \frac{1}{2}\left(p_{11} + p_{12}\right)(\varepsilon_x + \varepsilon_y)\Big) \quad (6)$$

And assume $\varepsilon_y = \varepsilon_x = -v\ \varepsilon_z$, where the v Poisson's ratio of the optical fiber, Then,

$$\frac{\Delta\lambda_{b,y}}{\lambda_{b0}} = (1 - \frac{n_0^2}{2}(p_{12} - v(p_{11} + p_{12}))_z \quad (7)$$

$$\Delta\lambda_b = (1 - p_e)\lambda_b\ {}_z \quad (8)$$

$${}_z = \frac{\Delta\lambda_b}{\lambda_b\ (1-p_e)} \quad (9)$$

${}_z$ is the applied strain, and p_e is the effective photo elastic coefficient, which is expressed as:

$$p_e = \frac{n}{2}[p_{12} - v_f(p_{11} + p_{12})] \quad (10)$$

Where $p_e \approx 0.22$ *10-6, $p_{11} \approx 0.113$, $p_{12} \approx 0.252$, $v_f \approx 0.16$.

The Bragg wavelength is a function of the refractive index of the fiber core and the grating period. If the grating is subjected to external perturbations, such as strain and temperature, the Bragg wavelength is changed. By measuring the wavelength change accurately, we can measure physical properties such as strain and temperature; this is the fundamental principle that allows the fiber Bragg grating to be used as a sensor [1].

Assume no stress loading (ε =0) and the shift of Bragg wavelength due to temperature is expressed as follows:

$$\Delta\lambda_b = 2\{n_{eff}\frac{\Delta\Lambda}{\Delta T} + \Lambda\frac{\Delta n_{eff}}{\Delta T}\}\Delta T \quad (11)$$

The Bragg wavelength changes when the temperature varies and this is related to change in the physical properties of the FBG as well as the change in refractive index and the grating period, as the result, the wavelength shifting can be determined due to temperature change ΔT [9]:

$$\Delta\lambda_b = \lambda_b(\alpha_f + \alpha_n)\Delta T = \lambda_b\beta\Delta T \quad (12)$$

Where $\alpha_f = \frac{1}{\Delta T}\Delta$ is the thermal expansion coefficient of the optical fiber ≈ 0.55*10-6 1/K for silica, and the $\alpha_n = \frac{1}{\Delta n_{eff}}\frac{\Delta n_{eff}}{\Delta T}$ represented the thermo-optic coefficient which varies between 3.0*10-6 and 8.6*10-6 1/K. The two coefficients αn, α_f were combined in one coefficient which is called the temperature coefficient β [10].

Non-uniform strain distribution causes non-uniform change of both the reflective index and grating period along the grating gauge and consequently changes the shape and split the reflect spectrum of the FBG. Some of authors used short grating length with an array of FBG by assuming uniformity of strain in each grating. However, this technique is limited by the physical conditions of the fabrication process [11].

III. Non- Uniform Strain and Temperature Distribution along Fiber Bragg Grating

When the strain distribution along the gauge of the FBG is non-uniform, the shape and the amplitude of the spectrum change split and brand the spectrum due to the stress concentrated in specific location of grating [3].

The index refraction effect n_{eff} of the optical fiber core is described by:

$$\delta n_{eff}(z) = \overline{\delta n_{neff}} - [1 + v\cos[\frac{2}{0}z + \phi(z)] \quad (13)$$

Where v is the fringe visibility, δn_{eff} and $\phi(z)$ are the spatial indexes change averaged over a grating period and the grating chirp respectively.

By using coupling mode theory, the first order differential equations describing the propagation mode through the grating in the z-direction are:

$$\frac{dR(z)}{dz} = i\acute{o}R(z) + iKs(z) \quad (14)$$

$$\frac{ds(z)}{dz} = -i\acute{o}s(z) - iKR(z) \quad (15)$$

R (z) and S (z) are the amplitudes of the forward and backward propagation modes, respectively, ó is the general

self-coupling coefficient as a function of the propagating wavelength λ, defined as:

$$\acute{o} = 2\pi\, n_{eff}\left(\frac{1}{\lambda} - \frac{1}{\lambda_b}\right) + \frac{2\pi}{\lambda}\,\overline{\delta n_{neff}} - \frac{1}{2}\,\acute{\phi}(z) \tag{16}$$

Where the $\acute{\phi}(z)$=dϕ/dz, and $\acute{\phi}(z) = 0$ for uniform grating, $\lambda_b = 2n_{eff}$ is the designed wavelength which would be changed when the grating is subjected to various strain condition. $k = \frac{\pi}{\lambda}\, v\, \overline{\delta n_{neff}}$, is the coupling coefficient, in which $\overline{\delta n_{neff}} = 1.131 * 10^{-4}$, and v ≈ 1.

The length of uniform grating is assumed to be L, so the limits of the grating is defined as (-L/2 ≤ z ≥ L/2), while the boundary condition of the uniform Bragg grating R (-L/2) =1 and S (L/2) = 0.

The reflectivity of the Bragg grating, calculated as a function of the wavelength as follow:

$$r(\lambda) = \left|\frac{S(-\frac{L}{2})}{R(-\frac{L}{2})}\right|^2 \tag{17}$$

The T-matrix is used to determine the reflectivity of the uniform Bragg grating under uniform or non-uniform strain. This method used different FBG properties, divided the grating gauge into M smaller section with uniform coupling properties, noted that the number of the sections M cannot be arbitrarily large since several grating period is required for large coupling, hence the M is constrained as:

$$M \leq \frac{2n_{eff}}{\lambda_b} L \tag{18}$$

By defining Ri and Si as field amplitudes after traversing the i_{th} grating section, the propagation through this uniform section can be described by:

$$\begin{bmatrix} Ri \\ Si \end{bmatrix} = Fi \begin{bmatrix} R_{i-1} \\ S_{i-1} \end{bmatrix} \tag{19}$$

Where

$$Fi = \begin{pmatrix} \cosh(\gamma_B \Delta_z) - i\frac{\delta}{\gamma_B}\sinh(\gamma_B \Delta_z) & -i\frac{K}{\gamma_B}\sinh(\gamma_B \Delta_z) \\ i\frac{K}{\gamma_B}\sinh(\gamma_B \Delta_z) & \cosh(\gamma_B \Delta_z) + i\frac{\delta}{\gamma_B}\sinh(\gamma_B \Delta_z) \end{pmatrix} \tag{20}$$

In which Δz is the length of each section. $\gamma_B = \sqrt{k^2 - \acute{o}^2}$, the T-matrix F for entire grating can be written as:

$$\begin{bmatrix} R(-\frac{L}{2}) \\ S(-\frac{L}{2}) \end{bmatrix} = F \begin{bmatrix} R(\frac{L}{2}) \\ S(\frac{L}{2}) \end{bmatrix} \tag{21}$$

where F= F_M, F_{M-1}, … , F_1.

The reflectivity of the entire grating is then calculated using (17). Fig. 1 shows the flowchart for the coupling mode theory and T-Matrix method that we have written in Matlab codes.

IV. Simulation of the Spectrum Reflection of the FBGs

To understand the reflected spectrum of the FBG corresponding to the strain distribution along the FBG, the simulation of the change in physical properties of the fiber sensor was performed as follows:

1. Change in the gauge length of the grating.
2. Change the reflective index of the grating.
3. Change in the period index of the fiber according to change in the strain loading.

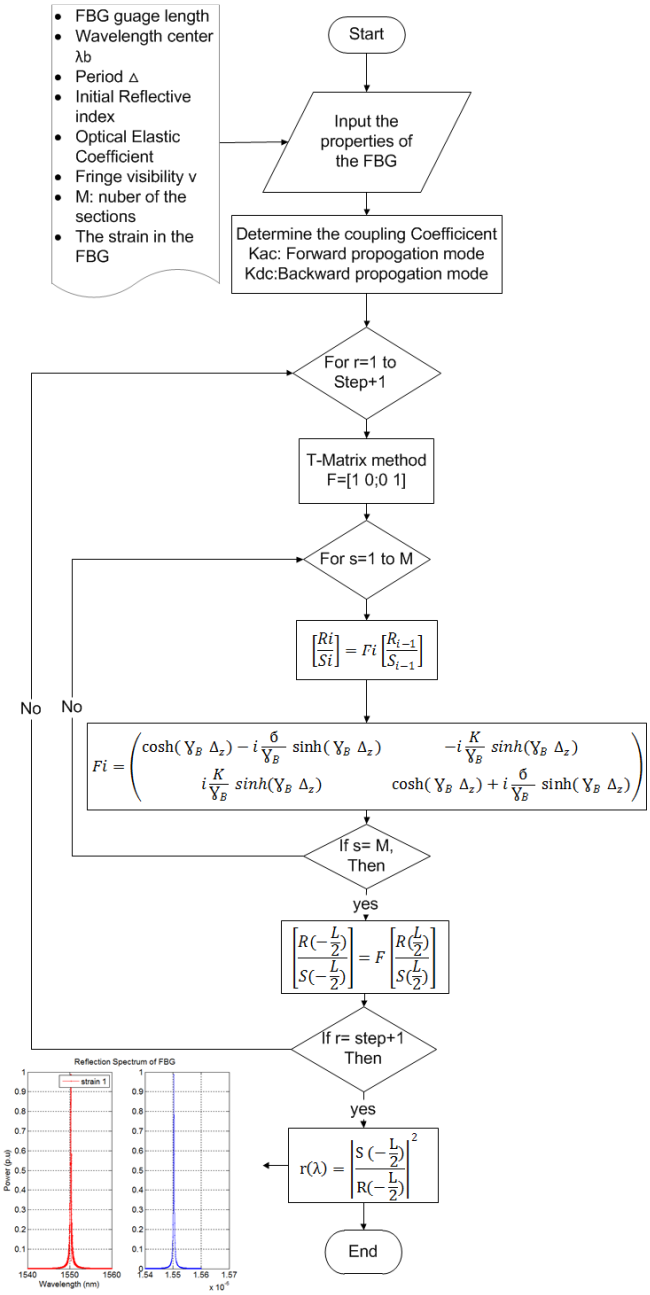

Fig. 1 Flowchart of FBG spectrum generation

For the change of the grating length in FBG, as the grating length increased the bandwidth of the reflected spectrum is decreased however the reflectivity of the spectrum increased. This means that the light passed through the grating gauge was reflected in each grating and the total reflectivity which increased as shown in Fig. 2. Simulation results for changing the grating length shows the split of the spectrum due non-

uniform strain distribution along the long grating FBG, for this reason, it's recommended to use the short grating FBG to overcome this Situation in the reflected spectrum.

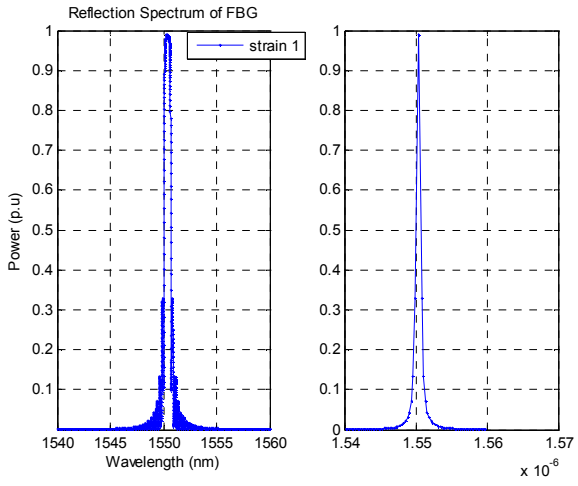

(a)

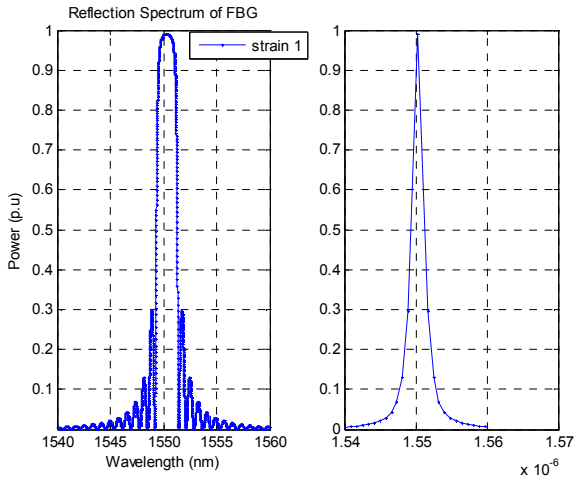

(b)

Fig. 2 Effect of the grating length, (a) grating length with 30mm, (b) grating length with 10mm

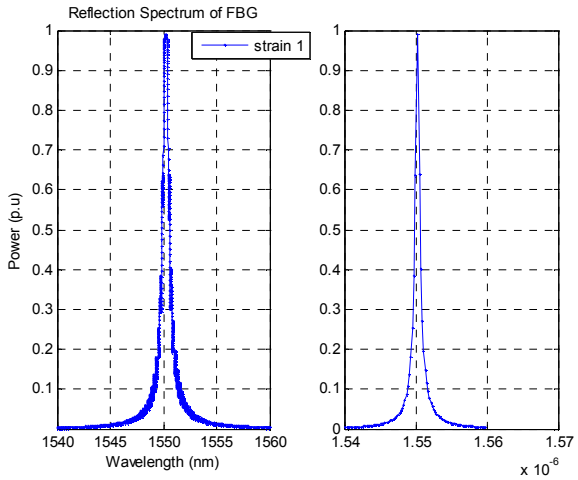

Fig. 3 Effect of the refractive index changing

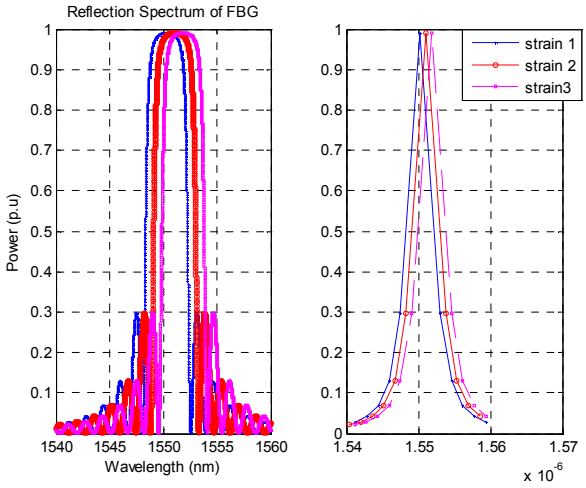

Fig. 4 Effect of the period index changing

The change in the local refractive index n_{eff} of the core caused distortion and split of the FBG's reflected spectrum and changed the amplitude of the reflectivity of the spectrum. This situation occurs when the refractive index along the grating gauge is changed with high gradating as shown in Fig. 3.

The change of the period Λ means the change in the distance among gratings due to the uniform strain along the fiber and hence the wavelength of the reflected spectrum will be getting shifted as shown in Fig. 4.

V. Numerical Modeling of DCB Specimens

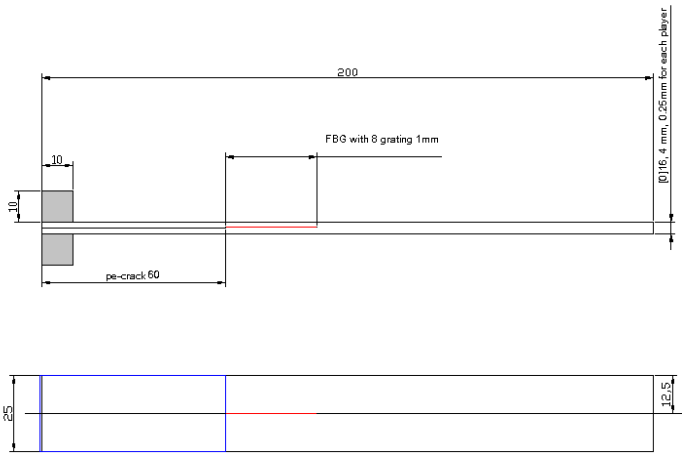

Fig. 5 DCB specimen dimensions used in numerical model.

Finite element method is used to provide the strain and the stress along the fiber Bragg sensor that is calculated by numerically measurements, and then converted it as a wavelength shifts from FBG reflected spectrum as illustrated in previous section.

The 3D model for unidirectional carbon fiber-reinforced epoxy composite having the stacking sequence $[0]_{16}$ with the properties E_{11}=128GPa, $E_{22}=E_{33}$=10GPa, G_{12}=5.7GPa, v_{12}=0.3, v_{23}=0.49, and also optical fiber properties E_f= 70GPa,

v_f =0.16, has been introduced to the DCB finite element model with specimen dimensions illustrated in Fig. 5.

Due to the small scaling of the FBG corresponding to composite structure, the problem was treated with two models; the global 3D half model with mesh of 15434 elements of type C3D8R for the composite material and COH3D8 for cohesive elements in which these elements was attributed traction-separation response which means that elements suffer stress along the crack opening. Firstly, the response of these elements before damage is linear–elastic behavior and after that when the damage occur these elements follows a softening behavior. This is obvious in the cohesive law described in Fig. 6.

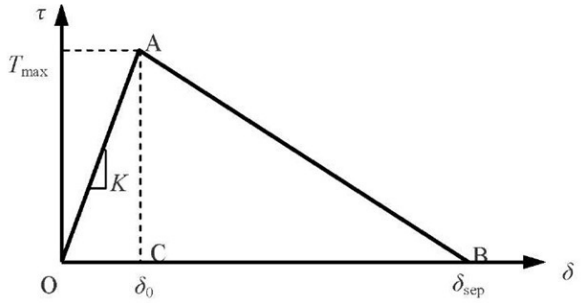

Fig. 6 Cohesive law describing cohesive elements behavior

Fig. 7 shows the refined mesh around the location of the crack tip. First, the global model is solved to obtain the specimen response under the applied loadings and boundary conditions.

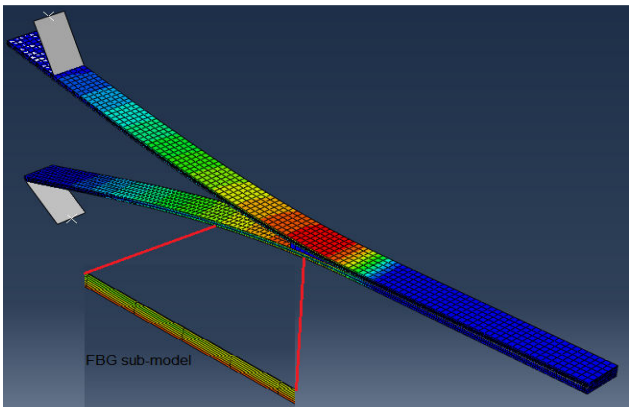

Fig. 7 The half global DCB model

In the sub-model analysis, the solution from the global model was applied to the FBG sub- model with a refined mesh of 4000 elements; the optical fiber was embedded above one layer distance from the delamination crack plane parallel to the direction of the reinforcing fibers [11]. The 3D model was used to determine the axial strain and investigating the effect of the transverse strain as shown in Fig. 8. After that, the strain was converted to corresponding wavelength shifting using (6) or (9) with respect to the elastic coefficient *Pe* of FBG as illustrated in Fig. 9.

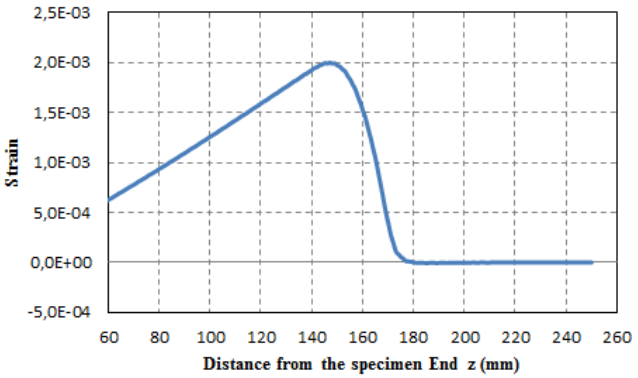

Fig. 8 Strain along the distance from specimen end z (mm)

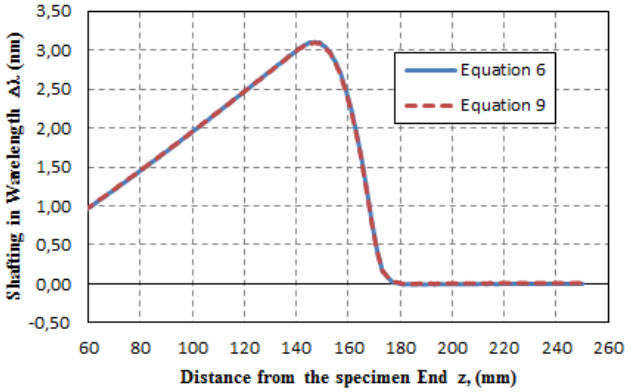

Fig. 9 Wavelength shifting from end z (mm) of specimen

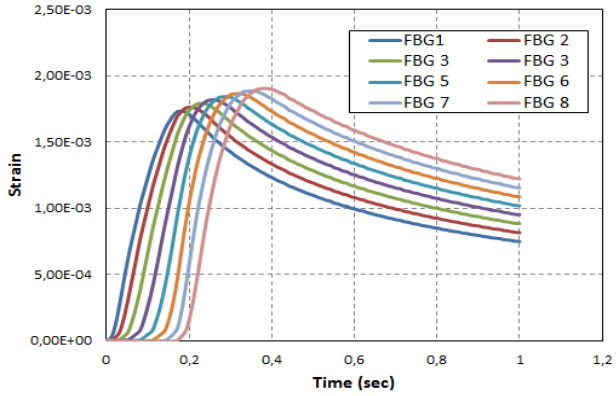

Fig. 10 Strain shift for an array of eight FBG_s during crack propagation (mm)

Fig. 10 demonstrates the axial strain measurements for an array of eight FBG sensors which are positioned along the FBG sub-model from crack initial a_0 toward the crack propagation. At a first, strain is not sense for any sensors, notes the elevation of the strain at the given position for each FBGs specifies crack length. The rising part of the curve indicates that the grating is located behind the crack tip and the max measurement of the each curve represents crack propagating under this grating gauge.

Wavelength shift measurements are calculated using (9) by converting the strain distribution form FBGs array, which is shown in Fig. 11.

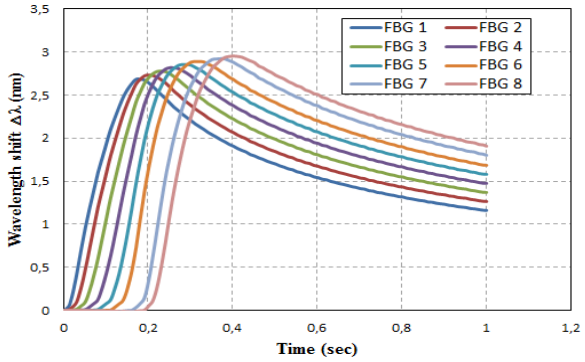

Fig. 11 Wavelength shift for an array of eight FBGs during crack propagate (mm)

Simulation of the reflection spectrum of FBGs array used to measure the longitudinal strain along the crack plane propagation is performed by converting the strain measurement for each FBG to correspond the reflected spectrum. Fig. 12 illustrated the reflection spectrum of FBGs array without strain.

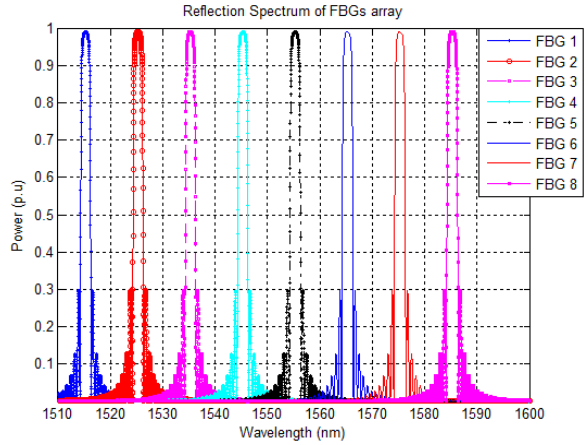

Fig. 12 Reflection spectrum of eight FBGs array without strain

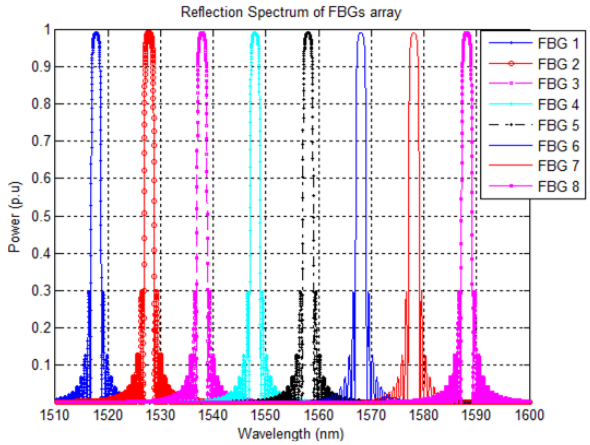

Fig. 13 Wavelength shifting of eight FBGs array under strain

Considering the assumption that homogeneous and uniform strain distribution in the FBG due to short grating length, then the spectrum keeps the same profile and only shifting wavelength in each grating occurs under axial strain. Fig. 13 represented the shifting in the wavelength of FBGs array identical to the maximum strain measurements for each sensor of Fig. 10.

VI. Conclusion

This paper investigated the simulation of the FBGs reflected spectrum using the coupling mode theory and T-matrix method and studied the changing effect of the physical properties of the FBG, such as the grating length, reflective index and grating period. The finite element model for mode-I delamination in DCB test was modeled in Abaqus code (software) to determine the axial strain along the FBG and transform it to the spectrum reflected program in the aim to convert it into wavelength shifting. By simulating two grating lengths (long grating and short grating array) we observed that the spectrum was split and distorted for the long grating due to non-uniform strain distribution, while for short grating gauges, the spectrum kept the same shape and only was shifted in its wavelength.

Acknowledgment

This research was funded by the ENSTA Bretagne Ecole Doctorate, France and the Ministry of Higher Education and Scientific Research, Iraq.

References

[1] L.Sorensen, The response of embedded FBG sensors to nonuniform strains in CFRP composites during processing and delamination, 2006.
[2] Measures, Raymod M., "Smart Composite Structure with Embedded Sensors," composite Engineering, vol. 2, no. 5-7, pp. 597-618, 1992.
[3] Hang-Yin Ling , Kin-Tak Lau , Wei Jin b, and Kok-Cheung Chan, "Characterization of dynamic strain measurement using reflection spectrum from a fiber Bragg grating," Optics Communications, vol. 270, pp. 25-30, 2007.
[4] S. Takeda, Y. Okabe, and N. Takeda, "Delamination detection in CFRP laminates with embedded small-diameter fiber Bragg grating sensors," Composites: Part A, vol. 33, pp. 971-980, 2002.
[5] L. Sorensen, J. Botsis, T. Gmu¨r, and J.¨l Cugnoni, "Delamination detection and characterisation of bridging tractionsusing long FBG optical sensors," Composites: Part A, vol. 38, pp. 2087-2096, 2007.
[6] B. D. Manshadi, A. P. Vassilopoulos, and J. Botsis, "A combined experimental/numerical study of the scaling effects on mode I delamination of GFRP," Composites Science and Technology, vol. 83, pp. 32-39, 2013.
[7] C.Schizas, S.Stutz, J. Botsis, and D.Coric, "Monitoring of non-homageneous strains in composites with embedded wavelength multiplexed fiber Bragg gratings: A methodological study," Composite Structures, vol. 94, pp. 987-994, 2012.
[8] D.H. Kang, S.O. Park, C.S. Hong, and C.G. Kim, "The signal characteristics of reflected spectra of fiber Bragg grating sensors with strain gradients and grating lengths," NDT&E International, vol. 38, pp. 712-718, 2005.
[9] C. M. Lawrence, D. V. Nelson, E. Udd, and T. Bennett, "A fiber optic sensor for transverse strain measurement" Experiment Mech, vol. 39, pp. 202-209, 1999.
[10] Othonos A., Kalli K, Fiber Bragg Gratings: Fundamentals and Applications in Telecommunications and Sensing, Artech House; Norwood, MA, USA, 1999.
[11] K. Peters, M. Studer, J. Botsis, A. Iocco, H. Limberger, and R. Salath, "Embedded Optical Fiber Bragg Grating Sensor in a Nonuniform Strain Field: Measurements and Simulations," Experimental Mechanics, vol. 41, no. 1, pp. 19-28, March 2001.